Exploring colloidal stability and migration dynamics through integrated photonic into aqueous black carbon dispersion

Jordan Gastebois, Anthony Szymczyk, Gilles Paboeuf, Florian Scholkopf, Véronique Vié, Arnaud Saint-Jalmes, Hervé Lhermite, Hervé Cormerais, Fabienne Gauffre, Bruno Bêche

Exploring colloidal stability and migration dynamics through integrated photonic into aqueous black carbon dispersion

J. Gastebois[a], A. Szymczyk[b], G. Paboeuf[c], F. Scholkopf[c], V. Vié[c,d], A. Saint-Jalmes[c], H. Lhermite[a], H. Cormerais[a,e], F. Gauffre[b], and B. Bêche[a]

[a]Univ Rennes, CNRS, IETR - UMR 6164, F-35000 Rennes, France
[b]Univ Rennes, CNRS, ISCR - UMR 6226, F-35000 Rennes, France
[c]Univ Rennes, CNRS, IPR - UMR 6251, F-35000 Rennes, France
[d]Univ Rennes, , UAR 2025 ScanMAT, F-35000 Rennes, France
[e]Centrale/Supelec, Campus de Rennes, F-35510 Cesson-Sévigné, France

ABSTRACT

This study investigates the migration and stability of colloidal suspensions through quasi-surfacic resonant analyses. The stability of colloidal suspensions is crucial in various industries such as food production, pharmaceutical formulations, and petroleum fields, where ensuring product quality and longevity is essential. The investigation presented here focuses on black carbon nano-powder dispersed in aqueous solutions, both with and without the incorporation of sodium dodecyl sulfate (SDS) surfactant. These solutions result in opaque and densely darkened mixtures, presenting challenges for conventional analytical techniques. To address this challenge, sensors based on integrated photonics are developed. These sensors consist of organic UV210 Micro-Resonators (MRs) shaped and fabricated via photolithography onto oxidized silicon substrates. The photonic chip is then integrated into a test platform where detection and signal processing are performed using a spectrometer and dedicated MATLAB codes to monitor optical measurements in real-time, crucial for investigate the dynamics of colloidal stability. Meticulous experimentations enable exploring the influence of black carbon nano-powder size and concentration on colloidal dispersion stability. The findings highlight the impact of the black carbon concentration on its migration and emphasize the anionic surfactant's effect on increasing stability by enhancing the repulsive forces between particles. These conclusions are corroborated with rheological plus zeta potential measurements to provide insights into determining colloidal dispersion stability and migration through optical resonant analysis.

Keywords: Integrated photonics and resonators, colloidal dispersion stability, soft matter, surface resonant signal processing, zeta potential measurement, rheology.

1. INTRODUCTION

Solutions stability is essential across various fields to ensure the product quality. In colloidal dispersions, an equilibrium between the electrostatic forces of dispersed particles results in a stable particle cloud. Changes in particles charges or in the host environment can alter these attractive or repulsive forces, leading to particle aggregation and a subsequent sedimentation. This process results in a non-homogeneous solution, which can negatively affect the product's lifetime. Maintaining product stability is a significant challenge in industries such as agro-alimentary,[1,2] or cosmetics.[3,4] Another difficulty arises from the nature of the product, which can be challenging to analyze. Opaque or dark substances are difficult to study using conventional techniques due to their tendency to absorb light during analysis.

Our solution is to develop a photonic chip capable of investigating these solutions through a quasi-surface resonant analysis. Integrated photonics are currently used in various applications, ranging from telecommunications to sensing. Optical cavity microresonators (MRs) can be localized on a photonic chip to serve as lab-on-chip sensing devices, incorporated into optical platforms. The interaction between the optical mode confined within

Further author information:
J. Gastebois : E-mail: jordan.gastebois@univ-rennes.fr
B. Bêche: E-mail: bruno.beche@univ-rennes.fr, https://www.ietr.fr/bruno-beche

the MRs and the environment, via an evanescent tail, has been utilized for detecting biochemical species[5] and for analyzing soft matter behavior.[6–8] More recently, silica nanoparticle sedimentation has been highlighted using resonant signals.[9] Our resonant element consists in a series of racetrack MRs made from an organic UV210 polymer resin, shaped by deep UV (DUV) photolithography onto an oxidized silicon wafer.[10,11] The resonances are excited by a superluminescent diode, and the quantified signal carries all the environmental information during the dynamic process. The Free Spectral Range (FSR) is directly related to the effective group index and to the propagation constant. The spectral variation resulting from the soft matter process under study is analyzed by dynamically tracking the FSR evolution using a spectrometer.

To investigate dark substances, we study the dispersion of black carbon nano-powder into aqueous medium. Black carbon consists of spherical particles resulting from the incomplete combustion of heavy hydrocarbons. These primary particles (10 nanometers) form indivisible aggregates of hundreds of nanometers.[12–14] Understanding their behavior into aqueous medium is essential for ensuring stability in liquid electrolytes, preventing sedimentation after charge and discharge cycles.[15] Therefore, we conduct investigations on the stability of two different black carbon nano-powder dispersions into acqueous solutions with varying black carbon concentration. The resonant signal analyses of a black carbon dispersion into a water plus a surfactant solution is corroborated to zeta potential measurement to develop the capability of our photonic chip to act as colloidal dispersion stability probe.

In the first part, we present the measurement protocol, detailing the preparation and characterization of the black carbon dispersion through SEM images and rheological analyses. We then briefly explain the materials processes as the optical test platform and the signal acquisition in the second part. The third part is dedicated to the resonant signal results, where we discuss the effect of black carbon concentration and size on the FSR variation. Finally, we link the FSR variation to colloidal dispersion stability using zeta potential measurements. The last part concludes this study.

2. EXPERIMENTAL SET UP AND PROTOCOLE MEASUREMENT

2.1 Sample preparation and black carbon characterization

To investigate dark substances, black carbon dispersions in aqueous medium are prepared. Two different black carbon nano-powders are considered. The first one, referred as "Powder 1," is sourced from Nanografi Nanotechnology (n°NG04EO7010)[16] and has been imaged and characterized by SEM analysis. The results show a size dispersion of 50 nm with aggregates around hundreds of nanometers (Figure 1.a). The second one, referred as "Powder 2," is sourced from Sigma-Aldrich (n°699632)[17] and has been characterized by both SEM and NTA (Nano Tracking Analysis). This powder has particle sizes below 100 nm and aggregates below 500 nm (Figure 1.b). The NTA distribution corresponds well with the SEM images(Fig. 1.c). The black curve represents the average measurement of three different analyses, while the red area indicates the maximum values from the three analyses. The particle sizes corresponding to each peak are indicated in blue.

Samples with different black carbon concentrations are prepared (Table 1). Black carbon nano-powders are dispersed in either deionized water or deionized water with a surfactant (the Sodium Docecyl Sulfate, SDS). The latter is prepared with a concentration of 4 mmol, which is below the critical micellar concentration of SDS (7-8 mmol at 20°C). The samples are then sonicated for 5 minutes using to break up agglomerates and achieve the most homogeneous solution possible.

Black carbon concentration (mg/mL)	**Sample name**
0.07	C_1
0.18	C_2
0.25	C_3
0.5	C_4

Table 1. Black carbon concentrations and their associated designations in the text.

The first analysis conducted was to determine the viscosity using an Anton Paar MCR 702e. A viscosity comparison was made between the dispersions at two concentrations (Figure 2.a) and with nano-powders 1 and

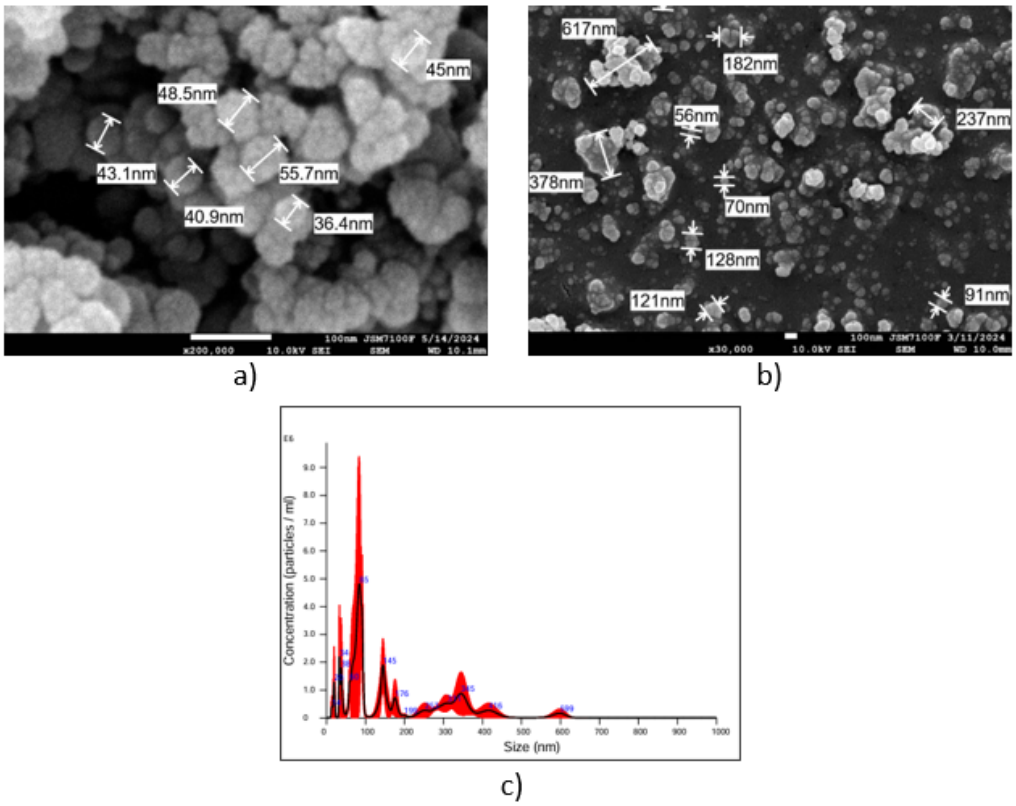

Figure 1. SEM images of black carbon nanopowder for: a) Powder 1, and b) Powder 2. c) NTA analysis of the size distribution for Powder 2, with the black curve representing the average of three measurements, the red curve showing the maximum values obtained, and the blue curve indicating the black carbon size corresponding to the peak.

2 at the same concentration (Figure 2.b). The C_3 dispersion has a higher viscosity than the C_4 dispersion but with no major differences. Higher concentrations increase the collision probability and viscosity. As the mean free path decreases with higher concentrations, the resistance encountered by the rheometer increases. However, in this case, the concentration differences are not significant enough to produce a noticeable change in viscosity. For different particle sizes, larger particles result in higher viscosity due to the shorter mean free path too.

2.2 Optical measurement set up

To explore the migration of black carbon dispersed in an aqueous medium, the substance is integrated into an optical test platform. The photonic chip, where the substance is placed in direct contact within a tank, is fabricated in a cleanroom. The optical cavity is composed of racetrack micro-resonators (MRs) coupled to an access taper waveguide made of an organic UV210 resin, developed using deep UV lithography on an oxidized silicon substrate (Figure 3.a). The fabrication processes have been detailed previously,[18] and the resulting resonant element with its geometrical parameters is shown in Figure 3.b.

The evanescent tail of an optical mode circulating inside the MRs serves as a probe to detect any variations and migrations in the tank containing the colloidal dispersion above the chip. To this end, a superluminescent diode (Superlum SLD 331 HP3) is used, with a central wavelength of $\lambda_0 = 795nm$ and a spectral width of $FWHM = 40nm$. The MR geometry induces a resonant condition $P.n_{eff}^{group} = m.\lambda_{res,m}$, with P the perimeter resonator, m an integer, n_{eff}^{group} the effective group index and $\lambda_{res,m}$ the resonant wavelenght. The Free Spectral Range (FSR) is defined as the difference between two consecutive resonant wavelengths and is directly related to the effective group index n_{eff}^{group}, which is related to the mode propagation constant $\beta = k_0 n_{eff}^{group}$ by $FSR =$

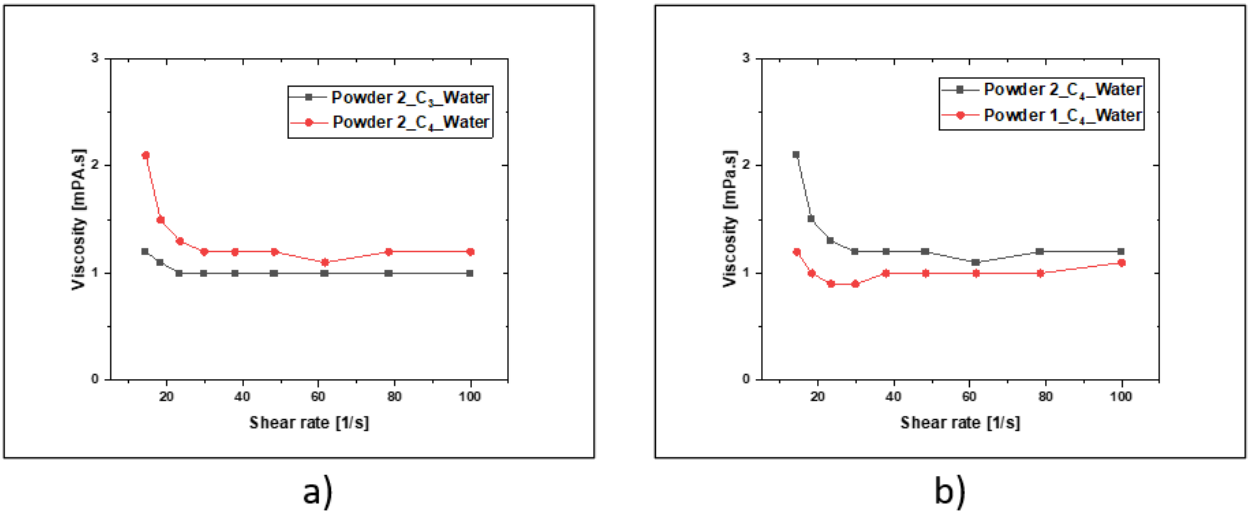

Figure 2. Viscosity measurements of black carbon dispersions in aqueous medium: a) Comparison of viscosity between two different concentrations for Powder 2, and b) Comparison of viscosity between Powder 1 and Powder 2 at the same concentration (C_4).

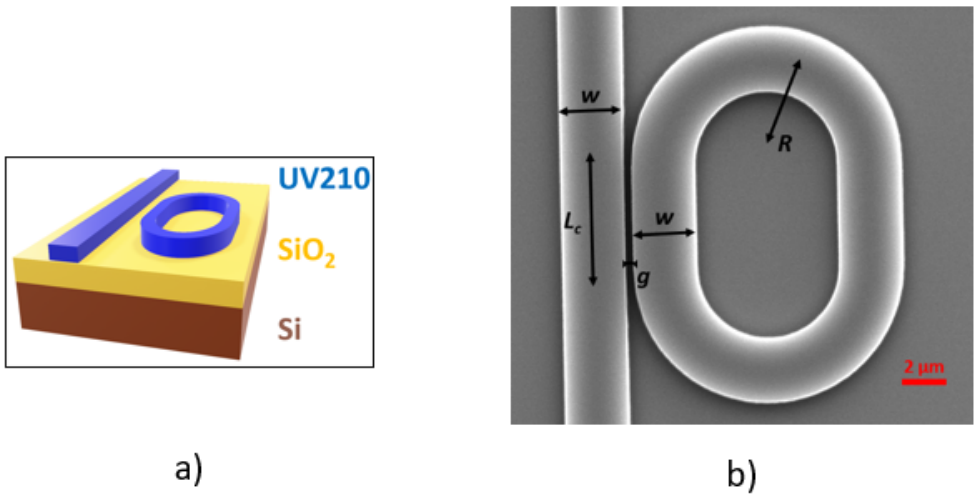

Figure 3. a) Schematic view of the resonant structure, featuring the organic resonant element developed on an oxidized silicon wafer. b) Scanning Electron Microscope (SEM) image of a racetrack micro-resonator (MR) coupled to a straight bus waveguide with R = 5 µm, L_c = 5 µm, w = 5 µm, and a gap of 400 nm.

$\frac{\lambda_0^2}{P.n_{eff}^{group}}$. The dynamic monitoring of the FSR evolution provides insights into the colloidal dispersion behavior over time. A dedicated MATLAB code enables data collection from a spectrometer (HR4000 from Ocean Optics) and performs real-time analysis to extract the FSR using Fast Fourier Transform (FFT) operations. The optical experimental setup is summarized in Figure 4.

3. RESULT AND DISCUSSION

3.1 Resonant analyses

A first approach involves considering the migration of black carbon nano-powder of different sizes but at the same concentration in water. For this purpose, a tank placed above the MRs is filled with 150 µL of water,

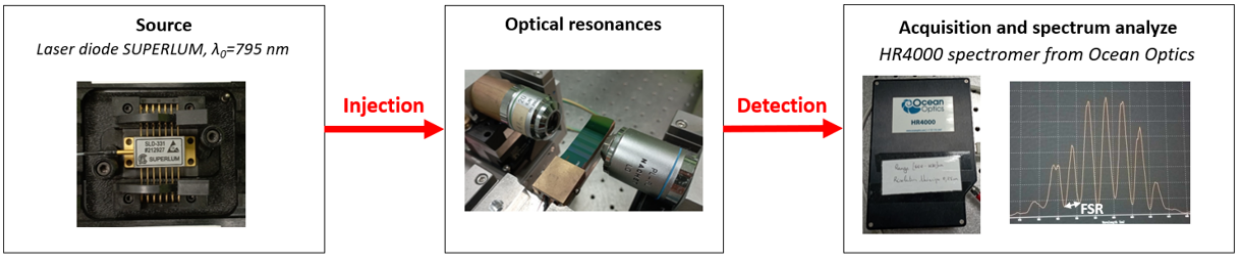

Figure 4. Schematic representation of the optical test platform, illustrating the setup from the broadband laser diode source (SUPERLUM) to the spectral analysis system (HR4000 spectrometer connected to a computer and controlled through a real-time MATLAB interface).

and black carbon is added to achieve the final concentrations presented in Table 1. The FSR measurements are obtained throughout the migration process under various conditions: Powder 1 at concentrations C_1, C_2, and C_4 (Figure 5), and Powder 2 at concentrations C_1, C_2, C_3, and C_4 (Figure 6).

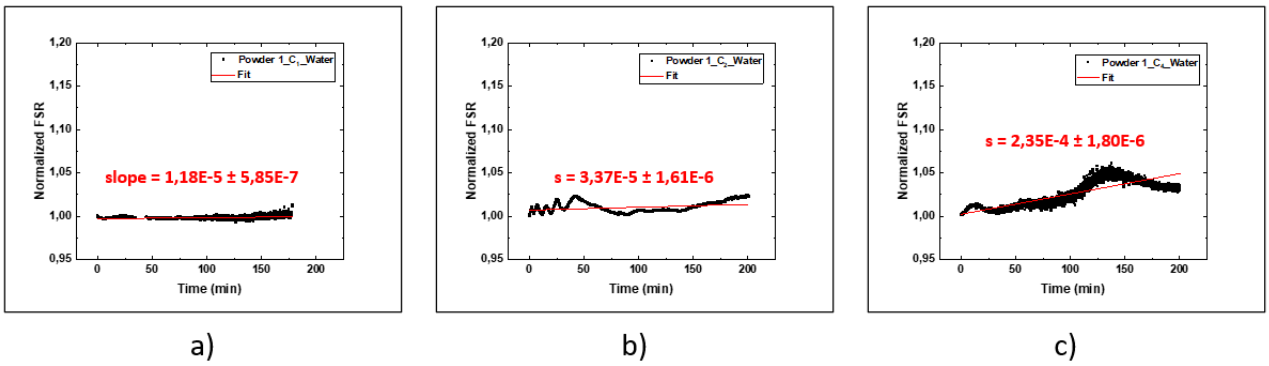

Figure 5. Plot of the normalized FSR evolution over time for three different concentrations of black carbon Powder 1: a) C_1, b) C_2, and c) C_4.

The initial observations on the migration and colloidal dispersion behavior can be made regardless of the black carbon powder size. For "Powder 1", the particle size is too small compared to the excitation wavelength, with an average size of approximately 50 nm, which corresponds to $\frac{\lambda}{15}$. At the lowest concentration, there is no noticeable FSR variation because the particles are too sub-lambda. As the black carbon concentration increases, variations in the dynamic evolution of the FSR can be observed, but these are attributed to the presence of agglomerates, which are more prevalent at higher concentrations. In contrast, for "Powder 2", the particle size is sufficient to detect migration (corresponding to FSR variation) at any black carbon concentration. An increase in FSR over time is detected, corresponding to sedimentation, as previously measured.[9,18] The sedimentation process end, as indicated by the stabilization of the FSR, takes approximately 200 minutes for all concentrations. The relative amplitude of FSR variation, which strongly depends on the intrinsic material properties, remains consistent for all the black carbon concentration (typically 1.15 times higher than the initial FSR value), indicating that the black carbon properties (permittivity) are unchanged in all the measurements. This consistency is further evidenced by plotting the FSR slope of sedimenting black carbon as a function of concentration (Figure 7). The lack of concentration effect on sedimentation can be correlated with the rheological measurements presented in Section 2.

Another observation can be made regarding the FSR oscillations visible at concentrations C_1 and C_2, which disappear at concentration C_3 for the powder 2 (Figure 6). When the black carbon solution is added to the tank filled with water, a composition gradient is present in the solution. This gradient, due to the Marangoni effect,[19] generates vortices in the solution, inducing movement of black carbon over the photonic chip, which manifests

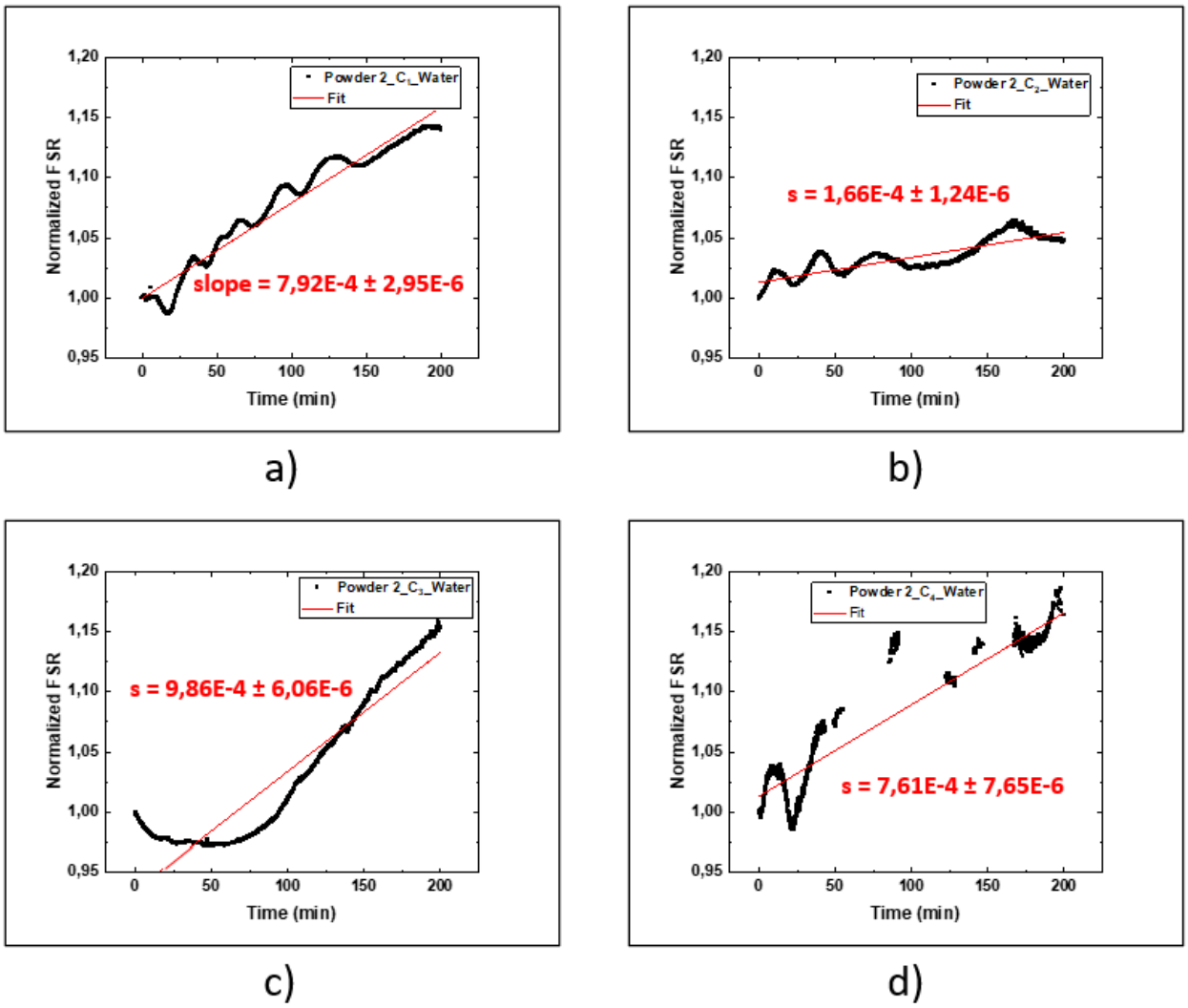

Figure 6. Plot of the normalized FSR evolution over time for four different concentrations of black carbon Powder 2: a) C_1, b) C_2, c) C_3, and d) C_4.

as FSR oscillations. As the concentration increases, particles have less space for displacement. The higher black carbon concentration corresponds to a decreased mean free path, resulting in less pronounced Marangoni oscillations. There appears to be a concentration threshold beyond which Marangoni oscillations no longer occur, as observed at concentration C_3 (Figure 6.c).

3.2 From a resonant signal analysis to colloidal dispersion stability measurement

To prevent particle agglomeration, a surfactant, Sodium Dodecyl Sulfate (SDS), is added to the black carbon solutions. As a result, there is no further FSR evolution, even over extended periods (Figure 8). The absence of FSR evolution indicates that sedimentation has been prevented and that the dispersion is stabilized. To corroborate this observation from the photonic experiments, zeta potential measurements[20] were conducted on the black carbon dispersions. Two samples at concentrations C_3 and C_4, both with and without SDS, were studied. The samples were diluted 100 times to reduce absorption, and 30 statistical measurements were taken for each (Figure 9).

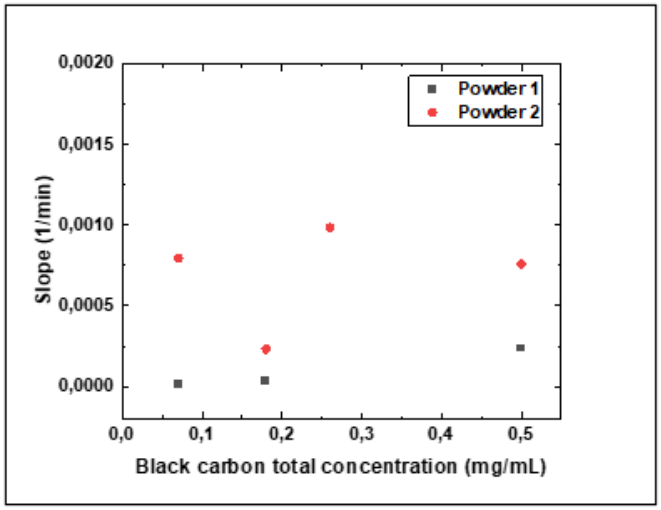

Figure 7. Plot of the FSR slope as a function of black carbon concentration for both Powder 1 and Powder 2.

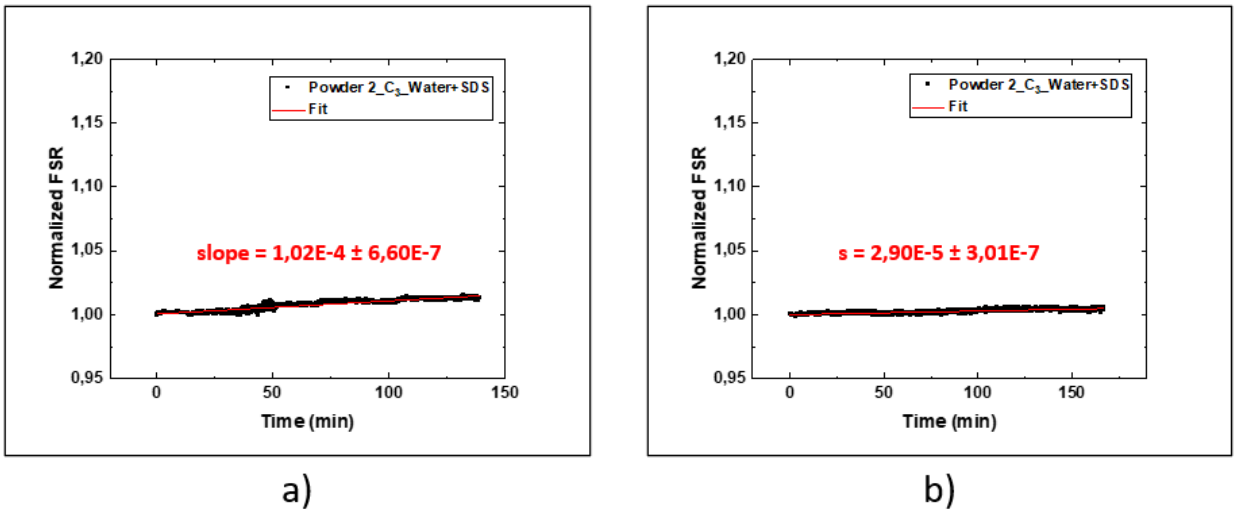

Figure 8. Plot of the normalized FSR evolution over time for black carbon Powder 2 dispersed in a water solution with SDS at concentration C_3.

It is noteworthy that the zeta potential for both concentrations doubles in the presence of SDS. The addition of an anionic surfactant modifies the charge of the black carbon particles. The black carbon absorbs the SDS anions, which then reside on the surface of the black carbon particles, resulting in a more negative zeta potential compared to the samples without SDS. With SDS, the dispersion exceeds the absolute threshold of 30 mV, which is known in the literature[21] as the stability threshold for colloidal dispersions. This confirms that our photonic chip is capable of detecting the stability of colloidal dispersions. The FSR slope can therefore be used as a tool to measure relative stability and to compare and determine which solution exhibits the greatest stability.

4. CONCLUSION

The investigation of opaque colloidal dispersion has been made possible using resonant principles through a 'lab-on-chip' photonic circuit. This circuit, developed in a cleanroom and composed of organic UV210 MRs, was placed in direct contact with black carbon dispersions in aqueous solutions. By monitoring the Free Spectral

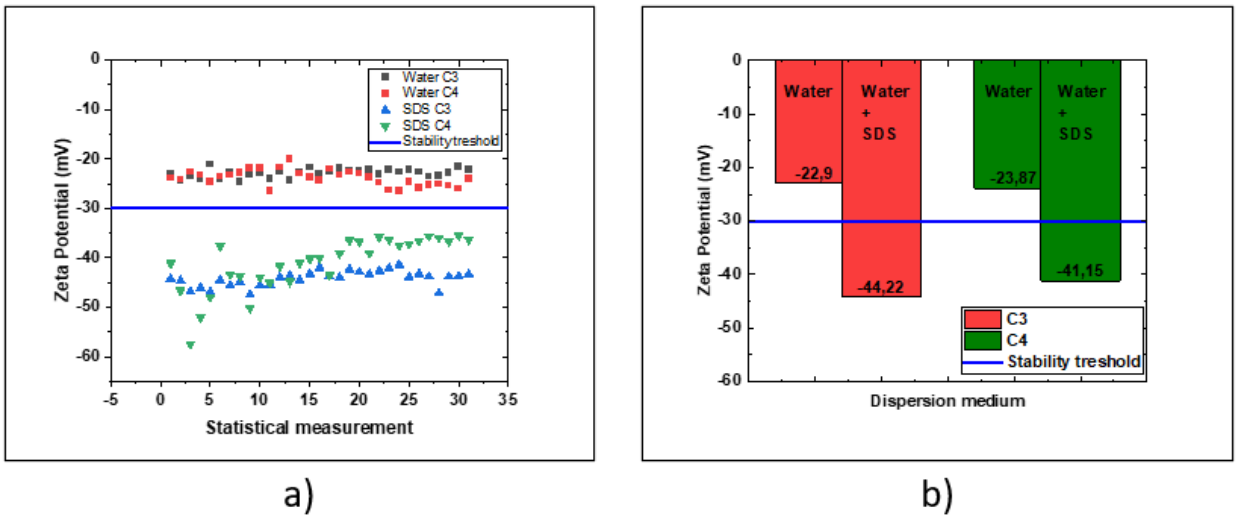

Figure 9. a) 30 zeta potential measurements were taken for 4 samples with and without SDS for concentration C_3 and C_4 diluted 100 times. b) Average value of the zeta potential. The colloidal dispersion stability threshold, defined at ±30 mV, is highlighted in both figures.

Range (FSR) signal throughout the process, we were able to explore the sedimentation effects occurring at various black carbon concentrations. A typical sedimentation time of 200 minutes was observed, indicated by the stabilization of the FSR. A concentration threshold was identified where Marangoni effects no longer occur, as evidenced by the absence of FSR oscillations.

The addition of an anionic surfactant limit black carbon agglomeration and thus prevent sedimentation, as clearly shown by a stabilization of the FSR over 150 minutes. This observation was further corroborated by zeta potential measurements, where these solutions exceeded the absolute zeta potential threshold of 30 mV, the known stability criterion for colloidal suspensions. Our photonic chips are therefore capable of determining product stability. By analyzing the relative evolution of the FSR, we can discriminate between solutions or products, identifying those that exhibit the greatest stability, a crucial factor for ensuring product quality and longevity.

Acknowledgments : The authors would like to thank the "Fondation d'Entreprise Grand Ouest" (BPGO) plus the "Fondation Rennes 1" for the financial support. The authors also thank the NanoRennes platform for the DUV process (https://www.ietr.fr/en/nr-nanorennes platform).

REFERENCES

[1] Grotenhuis, E. t., Tuinier, R., and de Kruif, C. G., "Phase Stability of Concentrated Dairy Products," *Journal of Dairy Science* **86**, 764–769 (Mar. 2003).

[2] Hyvärinen, H. K., Pihlava, J.-M., Hiidenhovi, J. A., Hietaniemi, V., Korhonen, H. J. T., and Ryhänen, E.-L., "Effect of Processing and Storage on the Stability of Flaxseed Lignan Added to Dairy Products," *Journal of Agricultural and Food Chemistry* **54**, 8788–8792 (Nov. 2006).

[3] Turek, C. and Stintzing, F., "Stability of Essential Oils: A Review," *Comprehensive reviews in food science and food safety* **12**, 40–53 (Jan. 2013).

[4] Zatz, J. L., "Applications of gums in pharmaceutical and cosmetic suspensions," *ACS Publications* **23**, 12–16 (May 2002).

[5] Densmore, A., Xu, D., Janz, S., Waldron, P., Lapointe, J., Mischki, T., Lopinski, G., Delâge, A., Schmid, J., and Cheben, P., "Sensitive Label-Free Biomolecular Detection Using Thin Silicon Waveguides," *Advances in Optical Technologies* (Jan. 2008).

[6] Li, Q., Garnier, L., Vié, V., Lhermite, H., Moréac, A., Morineau, D., Bourlieu-Lacanal, C., Ghoufi, A., Gaviot, E., Gicquel, E., and Bêche, B., "Sphingolipid Gel/Fluid Phase Transition Measurement by Integrated Resonance Probe Light," *Sensors & Transducers.* **225**, 41 – 48 (Oct. 2018).

[7] Castro-Beltrán, R., Garnier, L., Saint-Jalmes, A., Lhermite, H., Cormerais, H., Fameau, A. L., Gicquel, E., and Bêche, B., "Microphotonics for monitoring the supramolecular thermoresponsive behavior of fatty acid surfactant solutions," *Optics Communications* **468**, 125773 (Aug. 2020).

[8] Garnier, L., Lhermite, H., Vié, V., Pin, O., Liddell, Q., Cormerais, H., Gaviot, E., and Bêche, B., "Monitoring the evaporation of a sessile water droplet by means of integrated photonic resonator," *Journal of Physics D: Applied Physics* **53**, 125107 (Jan. 2020).

[9] Garnier, L., Gastebois, J., Lhermite, H., Vié, V., Saint-Jalmes, A., Cormerais, H., Gaviot, E., and Bêche, B., "On the detection of nanoparticle cloud migration by a resonant photonic surface signal towards sedimentation velocity measurements," *Results in Optics* **12**, 100430 (July 2023).

[10] Gouldieff, C., Huby, N., and Bêche, B., "Advantages of UV210 polymer for integrated optics applications: comparison of ridge and photoinscripted strip waveguide performances," *Journal of Optics* **17**, 125803 (Oct. 2015).

[11] Duval, D., Lhermite, H., Godet, C., Huby, N., and Bêche, B., "Fabrication and optical characterization of sub-micronic waveguide structures on UV210 polymer," *Journal of Optics* **12**, 055501 (May 2010).

[12] Jada, A., Ridaoui, H., and Donnet, J.-B., "Caractérisation des particules de noir de carbone dispersées en milieux aqueux et organique," in [*Énergie et formulation*], 78–83, EDP Sciences (Nov. 2005).

[13] Parant, H., Muller, G., Le Mercier, T., Tarascon, J. M., Poulin, P., and Colin, A., "Flowing suspensions of carbon black with high electronic conductivity for flow applications: Comparison between carbons black and exhibition of specific aggregation of carbon particles," *Carbon* **119**, 10–20 (Aug. 2017).

[14] "Noir de carbone (FT 264). Généralités - Fiche toxicologique - INRS."

[15] Guo, H., Wan, L., Tang, J., Wu, S., Su, Z., Sharma, N., Fang, Y., Liu, Z., and Zhao, C., "Stable colloid-in-acid electrolytes for long life proton batteries," *Nano Energy* **102**, 107642 (Nov. 2022).

[16] "Conductive Carbon Black Nanopowder, Size: 30 nm | Nanografi Nano Technology."

[17] "Carbon, mesoporous nanopowder, less than 500 ppm Al, Ti, Fe, Ni, Cu, and Zn combined | Sigma-Aldrich."

[18] Gastebois, J., Coulon, N., Cormerais, H., Levallois, C., Bêche, E., Esvan, J., Moréac, A., Lhermite, H., Garnier, L., and Bêche, B., "Low temperature PECVD processes for the fabrication of integrated symmetrical resonant UV210 organic/semiconductor structures," *Materials Today Communications* **39**, 109173 (June 2024).

[19] Marangoni, C., "Sul principio della viscosita' superficiale dei liquidi stabilito dalsig. J. Plateau," *Il Nuovo Cimento (1869-1876)* **5**, 239–273 (Dec. 1871).

[20] Kamble, S., Agrawal, S., Cherumukkil, S., Sharma, V., Jasra, R. V., and Munshi, P., "Revisiting zeta potential, the key feature of interfacial phenomena, with applications and recent advancements," *ChemistrySelect* **7**(1), e202103084 (2022).

[21] Lunardi, C. N., Gomes, A. J., Rocha, F. S., De Tommaso, J., and Patience, G. S., "Experimental methods in chemical engineering: Zeta potential," *The Canadian Journal of Chemical Engineering* **99**(3), 627–639 (2021).